Excitation-energy dependence of transient grating spectroscopy in β-carotene

Mitsuru Sugisaki,[1,*] Masazumi Fujiwara,[1] Selvakumar V. Nair,[2] Harry E. Ruda,[2] Richard J. Cogdell,[3] and Hideki Hashimoto[1]
[1]*Graduate School of Science, Osaka City University, 3-3-138 Sugimoto, Sumiyoshi, Osaka 558-8585, Japan*
[2]*Centre for Advanced Nanotechnology, University of Toronto, Haultain Building, 170 College Street, Toronto, Ontario, Canada M5S 3E3*
[3]*Division of Biochemistry and Molecular Biology, IBLS, University of Glasgow, Glasgow G12 8QQ, Scotland, United Kingdom*
(Received 30 March 2009; revised manuscript received 26 May 2009; published 16 July 2009)

Transient grating (TG) signals from β-carotene were measured at various excitation energies (wavelengths). Clear coherent oscillations with a period of a few tens of femtoseconds were observed when the excitation energy was tuned in the vicinity of the absorption edge. It was found that the TG signal is very sensitive to the excitation energy. When the TG signal is measured near the absorption maximum, following the coherent spike at the origin of the time axis, weak coherent oscillations are observed superimposed on a slowly varying background. The rise time of this slowly varying background is 0.4 ps and is followed by the slow decay with a 5 ps time constant. As the excitation energy is decreased the coherent oscillations become more prominent. The coherent oscillations and the slowly varying background become very weak again when the excitation energy is lower than the absorption edge. The TG signals were calculated using two sets of energy and Feynman diagrams to investigate possible pathways of the electronic internal conversion and vibronic decoherence processes. The modeling indicates that the vibronic coherence, initially established by pumping into the excited state S_2, instantaneously decays due to relaxation into an intermediate state S_x, which is located between S_2 and S_1. Possible interpretation of the nature of the S_x state is discussed.

DOI: 10.1103/PhysRevB.80.035118 PACS number(s): 82.53.Kp, 42.65.Re, 63.22.−m, 78.20.Bh

I. INTRODUCTION

Carotenoids play an essential role in photosynthetic light-harvesting complexes as both photoprotectors and accessory pigments. In antenna complexes, light energy absorbed by the carotenoids is transferred to (bacterio)chlorophylls. Interestingly, the energy transfer efficiencies of this process can reach nearly 100%.[1] It is clearly important to understand how these pigment molecules channel energy rapidly without the electronic excitation being dissipated wastefully into their surroundings.[2,3] Thermal dissipation of the electronic excitation in pigments takes place by vibronic coupling. In the case of antenna pigment-protein complexes this occurs through exciton-phonon interactions with the protein-binding sites.[4] Since the strengths of these interactions are determined by the potential-energy shapes of the ground and excited states, it is necessary to obtain detailed knowledge about the electronic and vibronic structures of photosynthetic pigments and surrounding proteins in order to investigate the dissipation processes.

In the present study we focus our attention on the ultrafast optical response of carotenoids in organic solvent. The electronic properties of carotenoids have been intensively investigated.[5] Their two low-lying singlet excited states, denoted by $2^1A_g^-$ (S_1) and $1^1B_u^+$ (S_2) in terms of C_{2h} symmetry labels, are responsible for most of their spectroscopic properties. In order to understand the mechanisms of the various energy transfer reactions in which they participate, information about the energies and lifetimes of the carotenoids' excited states is necessary. The internal conversion from S_2 to S_1 in β-carotene has been extensively investigated by means of various ultrafast spectroscopy techniques including transient absorption,[6–12] fluorescence up-conversion,[13–16] and femtosecond stimulated Raman spectroscopy.[17–20] Tavan and Schulten[21] presented a theoretical treatment of carotenoid excited states that suggested the presence of other potentially low-lying excited singlet states between S_2 and S_1 for carotenoids having more than nine conjugated double bonds. Following their predictions, several authors have presented experimental evidence in favor of such new states ($1B_u^-$ and $3^1A_g^-$) in various kinds of carotenoids, detected by means of resonance Raman spectroscopy and other spectroscopic techniques.[5,8,22–26] However, the involvement of these intermediate states is still controversial (see, for example, Refs. 18–20). It is necessary to employ powerful spectroscopic techniques to more reliably detect their possible presence.

With the availability of ultrashort femtosecond pulses, in addition to the electronic excited-state dynamics, it has become possible to monitor microscopic nuclear motion by various time-resolved spectroscopic techniques as coherent signals under impulsive excitation.[27] Ultrashort pulses have also been used to scrutinize the mechanics of decoherence, namely, the breakdown of time-reversal invariance of quantum evolution, which is inescapable eventuality in real systems.[28,29] Such decoherence processes have been investigated in various systems and, in general, coherence is lost due to coupling of the system to the environment provided by, for example, phonons, charge fluctuations in the surrounding materials, or the radiation field.[30–33] Since no system may be completely isolated from its environment, particular attention has to be paid to the influence of dissipation.

Recently, several authors have investigated vibronic coherent signals using ultrashort laser pulses to excite both photosynthetic pigments and pigment-protein complexes.[34–40] A central question when studying excitation-energy transfer in light-harvesting complexes is the balance between coherent and incoherent processes.[4] The most straightforward method to investigate this phenomenon would be to observe the decoherence processes of excitons. However this experiment is very difficult because an ul-

trashort laser with a 1 fs pulse width is necessary for the impulsive excitation of excitons in the visible region. We, therefore, have to consider other possible methods. Since the electrons and the core nuclei interact with each other in materials, we expect to observe the dissipation processes of the electronic excitation through the electron-phonon interaction or vibronic coupling. This phenomenon is reflected by the vibronic coherent oscillations. In photosynthetic organisms, carotenoid's absorptions cover the spectral region between 420 and 550 nm. Therefore it is interesting to investigate their coherent optical response while systematically changing the wavelength of the pump laser in this spectral region.

In this paper we investigate the excitation-energy (wavelength) dependence of the transient grating (TG) signals from β-carotene.[41] The experimental results are compared with a model based on a Brownian oscillation. In our previous study the TG signal obtained by the experiment was compared with the third-order polarizability $P^{(3)}$ calculated in the impulsive limit.[38,39] In the present study we relax this approximation and include the full temporal profile of the input pulses in the calculation of $P^{(3)}$. This is crucial for studying the excitation-energy dependence of the TG signal.

II. EXPERIMENTAL DETAILS

β-carotene was purchased from Wako Pure Chemical Industries, Ltd. and was purified by recrystallization from a benzene solution. For the optical measurements, β-carotene was dissolved in tetrahydrofuran (THF). The optical-absorption spectrum was recorded using a commercial spectrophotometer (JASCO, V-670). A 100-μm-thick optical flow cell sandwiched between 1-mm-thick windows was used for the TG measurement.[38] The sample concentration was adjusted so that the optical density is $\sim$1 at its absorption maximum. The excitation light source for the nonlinear optical measurements was constructed from a noncollinear optical parametric amplifier (NOPA) using a femtosecond Ti:sapphire regenerative amplifier (Spectra Physics, Hurricane). Details of the NOPA, together with the optical setup, have been reported elsewhere.[38] For the measurement of the TG signals, the compressed output beam from the NOPA was divided into three using pellicle membranes. The temporal separations between these pulses were set using computer-controlled linear translation stages (SIGMATECH, FS-1100PX). The pulse sequences used are shown in Fig. 1, where the center-to-center temporal separation of the first and second pulses is called the coherent period τ and that of the second and third pulses is the population period T. All the optical measurements were performed at room temperature. In order to tune the excitation wavelength, a slit was placed in the optical path of the prism compressor. The spectral width was narrowed as much as possible using the slit, but the temporal width was kept so that the cross-correlation signal is less than 20 fs. The pulse width of the excitation beam was optimized by measuring the autocorrelation trace of the pulses.

III. RESULTS AND DISCUSSION

A. Linear absorption spectrum and TG spectroscopy

The solid curve in Fig. 2 shows the absorption spectrum of β-carotene in THF. The absorption maximum of the 0-0 band of the S_0-S_2 transition is located at 20 600 cm^{-1}. The lowest optically allowed S_0-S_2 transition exhibits three characteristic peaks corresponding to the lowest three vibrational levels of the S_2 state. The energy spacing between the vibrational peaks of $\sim$1300 cm^{-1} is due to the combination of several vibrational modes.[5]

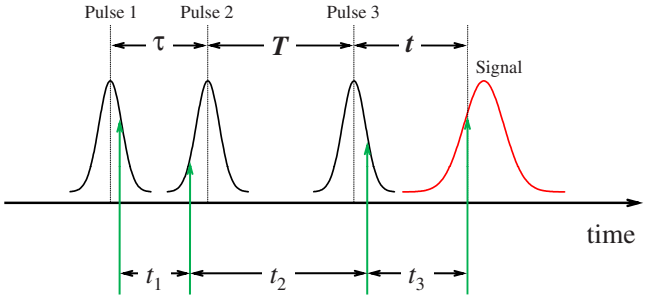

FIG. 1. (Color online) Definition of time variables. The temporal separation between the first two excitation pulses is coherent time τ. The population time T is the separation between the second and third excitation pulses.

Figure 3(a) shows the TG signals from β-carotene in THF measured at various excitation energies. The excitation energy of each TG trace is indicated by the arrows in Fig. 2, i.e., the excitation energy was tuned between the maximum of the 0-0 transition [curve A in Fig. 3(a)] and the absorption edge (curve D). The abscissa in Fig. 3(a) shows the population period T (temporal separation between pulses 2 and 3; see Fig. 1). The coherent period τ (temporal separation between pulses 1 and 2) is set to zero. In each TG signal in Fig. 3(a), after the coherent spike at T=0, coherent oscillations appear as superimposed on slowly varying components. It should be noted that the coherent spike of each curve has been truncated for clarity as the coherent oscillations are much weaker than the spike. The TG signal measured with excitation at the higher-energy side shows a large rise ($\sim$0.4 ps) followed by a slow decay component with a time constant of 5 ps [see curve A in Fig. 3(a)]. The rise compo-

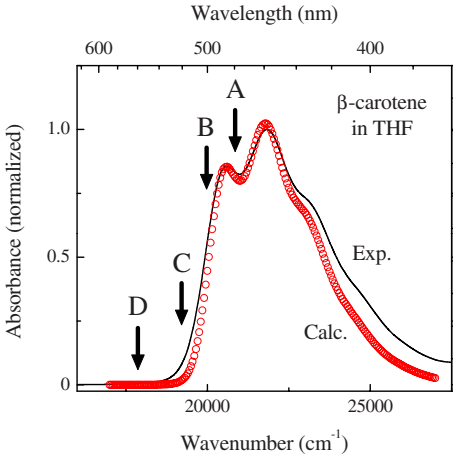

FIG. 2. (Color online) Absorption spectra of β-carotene in THF solution. Solid curve: experiment at room temperature. Circles: calculation. The arrows indicate the excitation energies for the TG signals shown in Fig. 3.

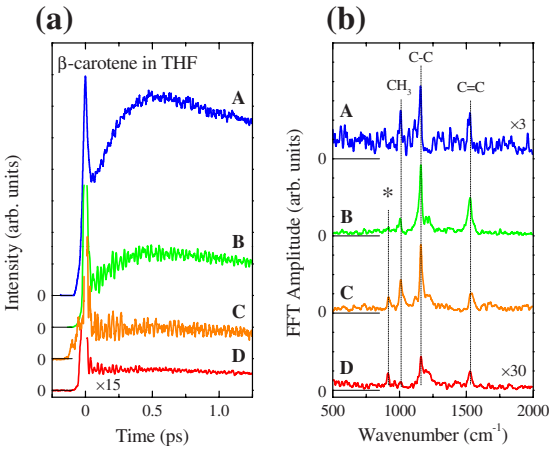

FIG. 3. (Color online) (a) Transient grating signals measured at various excitation energies which are indicated by the arrows in Fig. 2. The abscissa shows the temporal separation of the pulses 2 and 3 (the population period T). The coherent spike observed at the origin of the time is truncated. The signal becomes weak with the decrease in the excitation energy. Curve D is magnified by a factor of 15. (b) Fourier transform spectra of the curves shown in Fig. 3(a). The coherent spike and the slowly varying background are subtracted prior to the FFT analysis. The curves A and D are magnified by factors of 3 and 30, respectively, for clarity.

nent becomes less prominent as the excitation energy is decreased. The coherent oscillations are very clearly observed in curves B and C. The coherent oscillations and the slowly varying background become very weak when the excitation is set to the lower-energy side of the absorption edge (curve D).

The slowly varying background reflects the process of internal conversion, which will be discussed in detail in Sec. III B. The origin of the coherent oscillations can be understood as follows. We performed the fast Fourier transformation (FFT) analysis of the TG signals, as shown in Fig. 3(b). The coherent spike and the slowly varying background were subtracted from the TG signals prior to the FFT analysis. Several well-defined peaks are clearly seen in the FFT spectra. We can assign the origin of these peaks by comparing the resonance Raman spectrum of all-*trans*-β-carotene in THF with theoretical calculations such as normal-coordinate and the density-functional analyses.[42,43] The very intense peaks observed at 1522 and 1157 cm^{-1} correspond to the symmetric stretching modes of the C=C and C–C bonds, respectively. In addition, a very weak band seen at 1004 cm^{-1} is due to a methyl in-plane rocking mode. The peak marked by the asterisk (994 cm^{-1}) comes from the solvent THF. The coherent oscillations are less prominent when measured near the absorption edge compared to those measured on the higher-energy side (the amplitude of oscillations in curve D is more than one order of magnitude smaller compared to those of curves B and C).

B. Numerical calculation of the third-order polarizability

In the impulsive limit, the TG signals are simply given by the time integration of the total response function $R(t,T,\tau)$,

TABLE I. Parameters used for the numerical calculation. The parameters λ_B, ω_B, and γ_B are the reorganization energy, the frequency of the oscillator, and the damping constant of the low-frequency Brownian oscillation mode, respectively, which are introduced to define the spectral density as explained in Ref. 38. We note that the internal conversion rate Γ_{2x} is a variable as shown in Fig. 9.

	β-carotene
Δ_{in} (cm^{-1})	0
Γ (cm^{-1})	6
ω_B (cm^{-1})	250
γ_B (cm^{-1})	300
T (°C)	20
λ_B (cm^{-1})	560
ω_{eg} (cm^{-1})	22200
Γ_{20}^{-1} (fs)	1120
Γ_{x0}^{-1} (fs)	1120
Γ_{x1}^{-1} (fs)	120
Γ_{10}^{-1} (fs)	9000

$$S_{TG}(\tau,T) = \int_0^\infty dt |R(t,T,\tau)|^2 |\chi(t-\tau)|^2 \quad (1)$$

with

$$\chi(t) = \exp(-\Delta_{in}^2 t^2/2), \quad (2)$$

where $\chi(t)$ represents inhomogeneous dephasing, i.e., the total macroscopic polarization decays as the contributions of solvent and solute go out of phase.[44] The response function was calculated from the line broadening function $g(t)$ based on a Brownian oscillator model.[44] The line-broadening function that indicates the time evolution of the transition frequency correlation can be calculated from the spectral density $\rho(\omega)$.[45,46] The parameters used for the present calculation are the same as those used in our previous study[38] and are summarized in Table I. Using these parameters the linear absorption spectrum can well be reproduced as shown by the circles in Fig. 2.

In our previous studies, we found that the calculated TG signal under the impulsive limit reproduces the experimental results for β-carotene and its homologs measured near the absorption edge rather well.[38,39,47] In the present case, however, the experimental results clearly show an excitation-energy dependence (see Fig. 3). However, Eq. (1) does not have any dependence on the excitation energy (wavelength). This is not surprising as impulsive limit effectively assumes that the input pulses are infinitely broad in the frequency space. It is therefore necessary to perform a more rigorous calculation with the temporal envelopes of the incident pulses properly taken into consideration.

The TG signals along the phase-matched direction $\boldsymbol{k} = -\boldsymbol{k}_1 + \boldsymbol{k}_2 + \boldsymbol{k}_3$ can be calculated, in principle, using the following expression:[44]

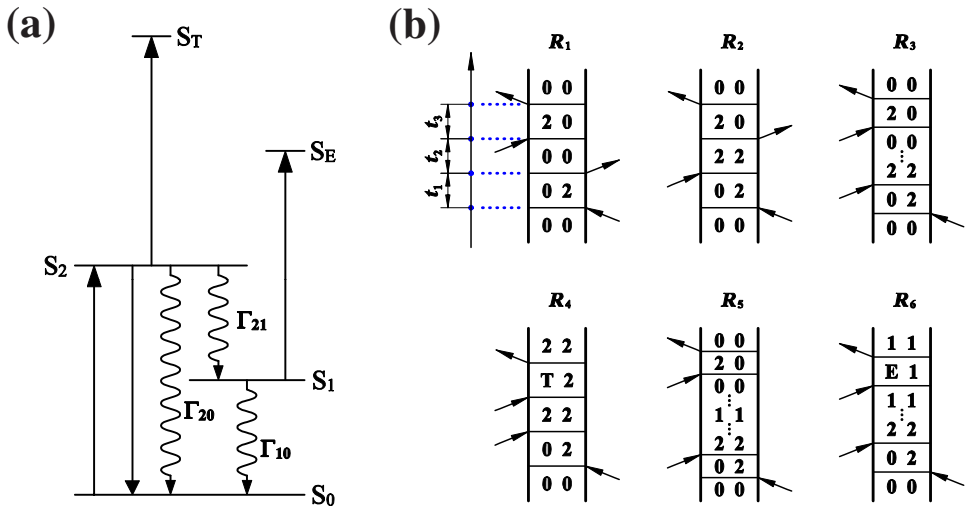

FIG. 4. (Color online) (a) Simple energy diagram of β-carotene. The transitions by optical pumping are indicted by the straight arrows, while the internal conversions are shown by the wavy arrows. S_T and S_E represent the two-photon and excited absorption states, respectively. (b) Double-sided Feynman diagrams used for the calculation. The symbols i (i=0, 1, 2, E, and T) indicate the S_i state. The diagrams R_1 and R_2 are the same as for a simple two-level system. The diagram R_3 includes the internal conversion directly from S_2 to S_0, while R_5 represents the relaxation from S_2 to S_0 through S_1. The diagram R_4 corresponds to the two-photon absorption process. The $S_E \leftarrow S_1$ absorption process (so-called "excited-state absorption") is represented in the diagram R_6. The vertically aligned dots indicate internal conversions.

$$S_{TG}(\tau,T) = \int_0^\infty dt |P^{(3)}(\boldsymbol{k},t)|^2 \tag{3}$$

with

$$P^{(3)}(\boldsymbol{k},t) \propto \int_0^\infty dt_3 \int_0^\infty dt_2 \int_0^\infty dt_1 R(t_3,t_2,t_1)\chi(t_3-t_1) \times E_3(t-t_3)E_2(t+\tau-t_3-t_2) \times E_1^*(t+\tau+T-t_3-t_2-t_1) \times \exp[i(\omega_3+\omega_2-\omega_1)t_3 + i(\omega_2-\omega_1)t_2 - i\omega_1 t_1]. \tag{4}$$

The definition of the time valuables is shown in Fig. 1. It may be noted that Eq. (4) contains information on the excitation energies $\hbar\omega_j$ (j=1, 2, and 3). Here $E_j(t)$ denotes the temporal envelope of the jth incident pulse. The excitation pulse shape was determined experimentally by means of cross correlation. Based on this measurement, we found that the temporal envelope of each optical pulse can be approximated by a Gaussian profile with a full width at half maximum of 18 fs for the numerical calculation.

We have calculated the TG signals using two sets of model energy diagrams and double-sided Feynman diagrams as shown in Figs. 4 and 5. The energy diagram shown in Fig. 4(a) represents the commonly accepted electronic structure of carotenoids, while that in Fig. 5(a) is another model that

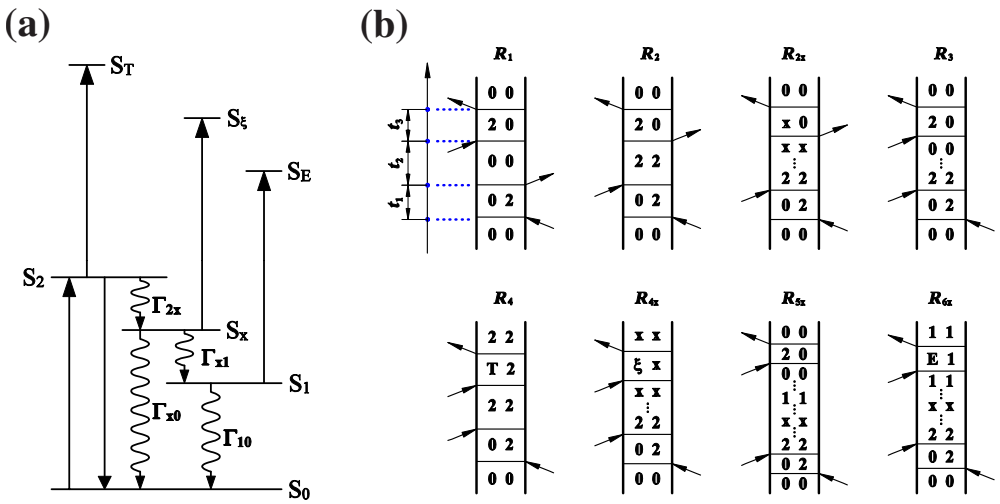

FIG. 5. (Color online) (a) Schematic energy diagram of β-carotene with an intermediate state S_x between S_1 and S_2. The excited-state absorption process $S_\xi \leftarrow S_x$ is also taken into consideration. (b) Double-sided Feynman diagrams based on the energy diagram shown in Fig. 5(a).

we employ for more detailed analysis, where an intermediate state S_x is introduced between S_2 and S_1. The energy diagram of carotenoids is usually described by analogy to all-*trans*-polyenes belonging to the C_{2h} point group [see Fig. 4(a)]. Since both of the ground state S_0 and the first low-lying excited singlet state S_1 have the same $^1A_g^-$ symmetry, a one-photon transition between these states is symmetry forbidden. The lowest optically allowed one-photon singlet state is S_2 and that has $^1B_u^+$ symmetry. In addition to these three states, we considered the involvement of S_T and S_E states in order to analyze the TG signals measured in our previous studies.[38,39] The excited state S_E is accessible through the $S_E \leftarrow S_1$ absorption process. The final state of a successive two-step absorption process via the S_2 state is denoted by S_T. The straight arrows in Fig. 4(a) represent the transitions allowed by the optical pumping and dumping, and the wavy arrows indicate the internal conversions. The decay rate between the S_i and S_j states is denoted by Γ_{ij}.

Figure 4(b) shows the double-sided Feynman diagrams used to calculate the TG signals, where the symbols i (i=0, 1, 2, E, and T) in these diagrams indicate the S_i state. The diagrams for the response functions R_1 and R_2 are the same as those used for a two-level system. Processes R_3, R_5, and R_6 involve the internal conversions, which are represented by the vertically aligned dots. For example, in process R_5, the population is formed by the first and second pump pulses in S_2 and then the population decays into S_0 via S_1 before the third pump pulse arrives. The process R_4 includes the excited-state absorption into the S_T state from S_2. The process R_6 represents the internal conversion from S_2 to S_1 followed by the $S_E \leftarrow S_1$ excited-state absorption.

In our previous studies,[38] the calculated model was simplified by making the following two assumptions: (1) in process R_4, in Fig. 4(b), the vibronic coherence is lost during the population period T and (2) the process R_6 was omitted since the transition energy of $S_E \leftarrow S_1$ is much smaller than that of $S_2 \leftarrow S_0$. In that study we found that the calculated signal under the impulsive limit reproduced well the TG signal measured at the isosbestic point, i.e., the energy where the bleaching of the ground state is canceled out by the excited-state absorption.[38] However, two questions remain: (1) why the vibronic coherence is *not* lost in the process R_2 during the population period T, while in the process R_4 the coherence is lost and (2) how justified is the neglect of the process R_6 in the calculation. These uncertainties come from oversimplification of the impulsive-limit calculation. We therefore calculated the TG signals over wide spectral range by a full consideration of the pulse width.

As shown in Eqs. (3) and (4), the TG signals can be calculated from the temporal evolution of the total response function R. The response function of each process is expressed by the exponent of a linear combination of the line broadening function $g(t)$, which indicates the time evolution of the transition frequency correlation.[44] The response function of each process shown in Fig. 4(b) can be expressed as

$$R_1 = |\mu_{20}|^4 \exp(i\omega_{20}t_1 - i\omega_{20}t_3)\exp[-g^*(t_1) + g^*(t_2) - g(t_3) - g^*(t_1+t_2) - g^*(t_2+t_3) + g^*(t_1+t_2+t_3)], \quad (5a)$$

$$R_2 = |\mu_{20}|^4 n_2 \exp(i\omega_{20}t_1 - i\omega_{20}t_3)\exp[-g^*(t_1) + g(t_2) - g^*(t_3) - g^*(t_1+t_2) - g(t_2+t_3) + g^*(t_1+t_2+t_3)], \quad (5b)$$

$$R_3 = |\mu_{20}|^4 r \exp(i\omega_{20}t_1 - i\omega_{20}t_3)\exp[-g^*(t_1) - g(t_3)], \quad (5c)$$

$$R_4 = |\mu_{20}|^2|\mu_{T2}|^2 n_2 \exp(i\omega_{20}t_1 - i\omega_{T2}t_3)\exp[-g^*(t_1) - g(t_2) - g(t_3) + g^*(t_1+t_2) + g(t_2+t_3) - g^*(t_1+t_2+t_3)], \quad (5d)$$

$$R_5 = |\mu_{20}|^4 (n_0 - r)\exp(i\omega_{20}t_1 - i\omega_{20}t_3)\exp[-g^*(t_1) - g(t_3)], \quad (5e)$$

$$R_6 = |\mu_{20}|^2|\mu_{E1}|^2 n_1 \exp(i\omega_{20}t_1 - i\omega_{E1}t_3)\exp[-g^*(t_1) - g(t_3)], \quad (5f)$$

where μ_{ij} and ω_{ij}, respectively, represent the transition dipole interaction and frequency between the S_i and S_j states and n_i indicates the population of the S_i state. The mathematical expressions for n_i and r have been given in Ref. 38. Equation (5) shows the response functions of the pulse sequences 1-2-3. The response functions of other pulse sequences were simply calculated in the same way. The most important aspect in the present analysis is that the processes given by R_2 and R_4 contain the exponent $g(t_2)$, which means that the vibronic coherence is preserved during the population period T. Equation (5) should be compared with Eq. (7) in Ref. 38. In the present calculation R_6, representing the $S_E \leftarrow S_1$, is also included in the total response function $R(t_3,t_2,t_1)$,

$$R = R_1 + R_2 - (R_3 + R_4 + R_5 + R_6). \quad (6)$$

By employing the spectral density $\rho(\omega)$, the line broadening function $g(t)$ at temperature T can be expressed as[48]

$$g(t) = -\frac{i\lambda t}{\hbar} + \int_0^\infty d\omega\ \rho(\omega)\coth\left(\frac{\hbar\omega\beta}{2}\right)(1-\cos\omega t) + i\int_0^\infty d\omega\ \rho(\omega)\sin\omega t, \quad (7)$$

where $\beta = 1/k_BT$ and k_B is the Boltzmann constant. The renormalization constant λ is given by[48]

$$\lambda = \hbar\int_0^\infty d\omega\ \omega\rho(\omega), \quad (8)$$

which represents the solvation reorganization energy.

The TG signals at the various excitation energies can be readily calculated using the Feynman diagrams shown in Fig. 4(b) and the total response function in Eq. (6). The calculated TG curves are shown in Fig. 6(a), where from top to bottom the excitation frequency decreases. The parameters used for the calculation are the same as those used in Ref. 38, which are summarized in Table I. For simplicity we did not include the coherent spike in the calculation. Over the whole spectral region examined the calculated curves do not reproduce the experimental results. As one can see from Eq. (4) the exact

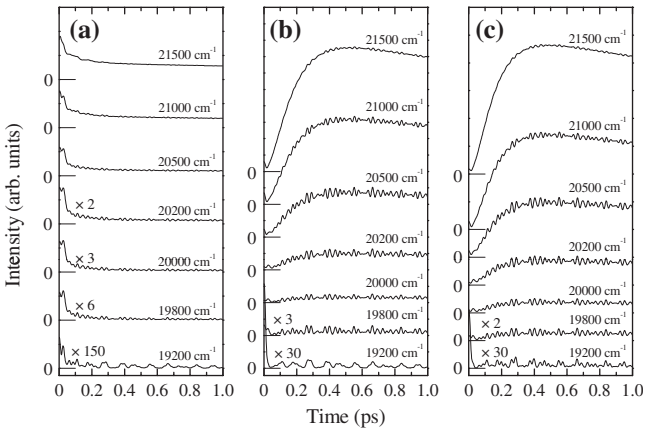

FIG. 6. TG signals at various excitation energies calculated using the diagrams shown in (a) Fig. 4 (without an intermediate state) and (b) Fig. 5 (with an intermediate state). The experimental results are qualitatively reproduced when the intermediate state S_x is introduced into the calculation. (c) Excitation-energy dependence of TG signals without including the excited-state absorption process $S_E \leftarrow S_1$. The other response functions are the same as those shown in Fig. 5.

expression of the third-order polarization involves the response function R and excitation pulse shape $E_j(t)$. Since we have already included the most realistic shape of the excitation pulses in the calculation, the most probable origin of the discrepancy between the experimental result and calculation of the TG signals comes from the inappropriate choice of the response function. Since the response function is directly determined by the energy level structure, we conclude that the model shown in Fig. 4(a) is insufficient to account for the experimental data.

As discussed by several authors, several intermediate states between S_2 and S_1 have been postulated (see, for example, Refs. 5 and 22–26). In the following we consider whether inclusion of an intermediate state allows the calculated signals to reproduce the experimental data. We introduced an intermediate state S_x between S_2 and S_1 as shown in Fig. 5(a) (the possible origin of S_x is discussed later). In this model, the excited-state absorption process from S_x to S_ξ is also taken into consideration. The double-sided Feynman diagrams for this model are shown in Fig. 5(b). The population initially excited into the state S_2 by optical pumping instantaneously decays into S_x and this process is considered in R_{2x}, R_{4x}, R_{5x}, and R_{6x}. This means that the vibronic coherent oscillations initially excited in the S_2 state decay before the transition into S_T occurs. The mathematical expressions of these response functions are given by

$$R_{2x} = |\mu_{20}|^2 |\mu_{x0}|^2 n_x \exp(i\omega_{20}t_1 - i\omega_{x0}t_3)\exp[-g^*(t_1) - g^*(t_3)], \tag{9a}$$

$$R_{4x} = |\mu_{20}|^2 |\mu_{\xi x}|^2 n_x \exp(i\omega_{20}t_1 - i\omega_{\xi x}t_3)\exp[-g^*(t_1) - g(t_3)], \tag{9b}$$

$$R_{5x} = R_5, \tag{9c}$$

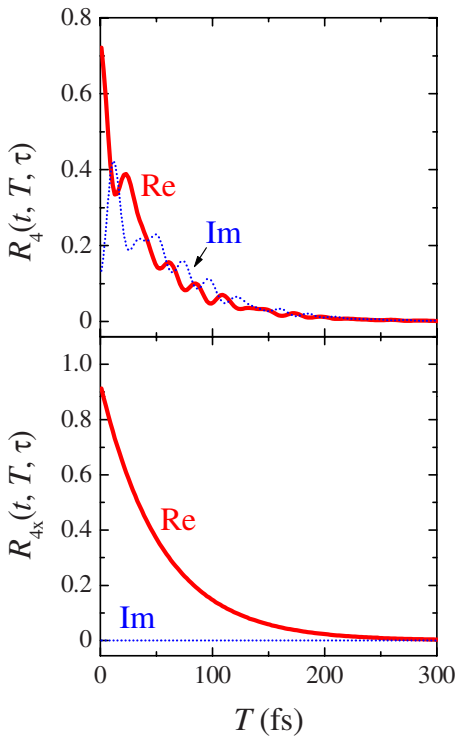

FIG. 7. (Color online) Temporal evolution of the response function for process $R_4(t,T,\tau)$ (top) and $R_{4x}(t,T,\tau)$ (bottom) as a function of population period T. The solid (dotted) curves show the real (imaginary) part. Here, the coherent periods τ and t are set to 1 fs.

$$R_{6x} = R_6. \tag{9d}$$

In the present case, the processes given by R_{2x} and R_{4x} do not hold the vibronic coherence during the population period T because of the internal conversion process from S_2 to S_x. The mathematical expression of the response function R_3 remains the same even when S_x is included. Therefore, the total response function is given by

$$R = R_1 + R_2 + R_{2x} - (R_3 + R_4 + R_{4x} + R_{5x} + R_{6x}). \tag{10}$$

In the process R_3, the internal conversion from S_2 (not from S_x) to S_0 is considered because optical absorption from S_0 to S_x has not been observed. This means that the transition dipole moment μ_{x0} is very small in which case R_{2x} may be neglected [see Eq. (9a)]. In the case of instantaneous decay from S_2 to S_x, the contribution of the process R_4 becomes very small because the population in S_2 decays immediately after the pump. Therefore, the influence of the existence of the S_x state is mainly reflected in processes R_4 and R_{4x} [see Eqs. (6) and (10)]. Figure 7 shows the temporal profiles of processes R_4 and R_{4x}. As expected, the vibronic oscillations coupled to the electronic excitation are seen in process R_4, while the real part of process R_{4x} monotonically decays because of instantaneous dephasing of vibronic oscillations.

The calculated TG signals, using the diagrams shown in Fig. 5, reproduce the details of the experimental results very well as shown in Fig. 6(b), where from top to bottom the excitation frequency decreases. We assumed that the relaxation from S_2 to S_x is instantaneous for simplicity. The tran-

sition energy $\hbar\omega_{\xi x}$ from S_x to S_ξ is set to 22 200 cm^{-1}, which is the same as that from S_2 to S_T. The TG signal shows a large rise (~0.4 ps) followed by a slow decay component when measured at the higher-energy side [see the 21 500 and 21 000 cm^{-1} curves in Fig. 6(b)], which is consistent with curve A in Fig. 3(a). As the excitation energy decreases, the coherent oscillations become prominent [the 20 500 and 20 200 cm^{-1} curves in Fig. 6(b)], which should be compared with curves B and C in Fig. 3(a). When the excitation energy is very low [the 20 000–19 200 cm^{-1} curves in Fig. 6(b)], the dip around 50 fs is less prominent and the slowly varying background monotonically decays. This is again consistent with experimentally observed curve D in Fig. 3(a). All these agreements between the experiment and calculation over the inspected spectral range support the model that includes the additional intermediate state. We note that we also calculated the TG signal by changing the transition energy $\hbar\omega_{\xi x}$ from 20 200 to 24 200 cm^{-1}; however, significant improvement of the fitting was not attained.

In spite of the encouraging agreement between the calculation and experiment, there are some significant quantitative discrepancies as well. It is important to discuss possible reasons for these differences. The calculated TG signals below 19 800 cm^{-1} in Fig. 6(b) are very weak, while curve C in Fig. 3(a), measured at 19 200 cm^{-1}, shows clear coherent oscillations and a slowly varying background. As seen in Fig. 2, it is difficult to have a good agreement between the model calculation and experiment near the absorption edge. In this spectral region, the absorption coefficient and thus the optical susceptibility change very rapidly. Therefore even small changes in parameters have a large effect on the calculated signal in this region. We note that the calculated absorption edge is slightly shifted toward the higher-energy side compared to the experimental result. From the absorption maximum of the 0-0 transition to the absorption edge on the lower-energy side, the rapid decrease in optical susceptibility seen in the calculation results in the rapid decrease in the intensity of the TG signal [see Fig. 6(b)]. In order to obtain better agreement between the calculated absorption spectrum and experiment, it might be necessary to include a partially optically allowed electronic level slightly below the absorption edge of the S_2 state.[23,49] However, we leave this issue as a subject of future study since the validity of this assumption has to be carefully considered.

As mentioned above, the TG signal measured on the lower-energy side of the absorption edge [curve D in Fig. 3(a)] shows a less prominent rise of about 0.4 ps compared to those measured on the higher-energy side [curves A and B in Fig. 3(a)]. This is consistent with the calculated TG signal. However, the calculated signal has a much weaker slowly varying background in comparison to the experimentally measured one. In order to clarify the reason for this, we measured the TG signals while changing the spectral shapes of the excitation pulses. The thin and thick solid curves in Fig. 8(a) show the spectra of the excitation pulses used for this experiment. The position of the edge on the lower-energy side is the same in both spectra, but the higher-energy side of curve A was cut using the slit set in the compressor of the NOPA. The compression of these pulses was optimized at 17 860 cm^{-1} as indicated by the arrow. Curve A in Fig. 8(b) is the TG signal measured using pulse A shown in Fig. 8(a), which is the same as curve D in Fig. 3(a). The TG signal B was measured using the pump pulse B and shows a clear dip around 50 fs and a slow rise of about 0.4 ps. This feature of the slowly varying background is similar to that observed in the TG signals measured at the higher-energy side [see curves B and C in Fig. 3(a)]. Therefore, we conclude that the significant amplitude of the slowly varying background observed in the experiment reflects the spectral broadening of the pump pulse. During the last decade, the availability of broadly tunable, few-optical cycle, light pulses has pushed the temporal resolution of ultrafast laser spectroscopy down to the sub-10 fs domain. Our results suggest that the spectral shape must be properly considered when trying to simulate experimental data such as the TG signals obtained in the present study.

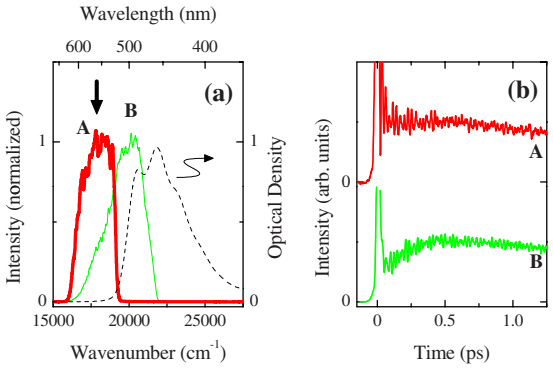

FIG. 8. (Color online) (a) Solid curves: spectra of NOPA. The pulses are compressed at the energy indicated by the arrow. Dashed curve: absorption spectrum of β-carotene. (b) TG signals measured under the excitation using pulses A and B shown in Fig. 8(a). The slowly varying background shows clear rise of about 0.4 ps when the spectral width of the pump pulse extends to the absorption edge.

It is interesting to consider TG signals calculated using other possible parameters. Figure 6(c) shows the TG signals *without* including process R_{6x}, i.e., the diagrams shown in Fig. 5 are used but the excited-state absorption $S_E \leftarrow S_1$ is omitted. The overall shapes shown in Fig. 6(c) agree well with those shown in Fig. 6(b). This result indicates that the involvement, the $S_E \leftarrow S_1$ process, is negligible in the spectral region investigated in the present study. In our pervious study, the TG signal under the impulsive limit was calculated and good agreement between the experiment and the calculation was obtained even when the exited-state absorption $S_E \leftarrow S_1$ was neglected.[38,39] Our present calculations indicate that the TG signal is very sensitive when the excitation energy resonates with the singlet electronic levels. In the present case, the energy separation between $S_E \leftarrow S_1$ (16 600 cm^{-1}) is much smaller than the excitation energy (21 500–19 200 cm^{-1}). This is the reason why our previous calculation in the impulsive limit reproduced the experimental results so well.

Figure 9 shows the excitation-energy dependence of the TG curves calculated using various finite values of Γ_{2x}^{-1}. Here Γ_{x1}^{-1} is set to 120 fs because this parameter represents the rise of the S_1 state and we keep this parameter constant throughout the following calculation. The coherent spike is not in-

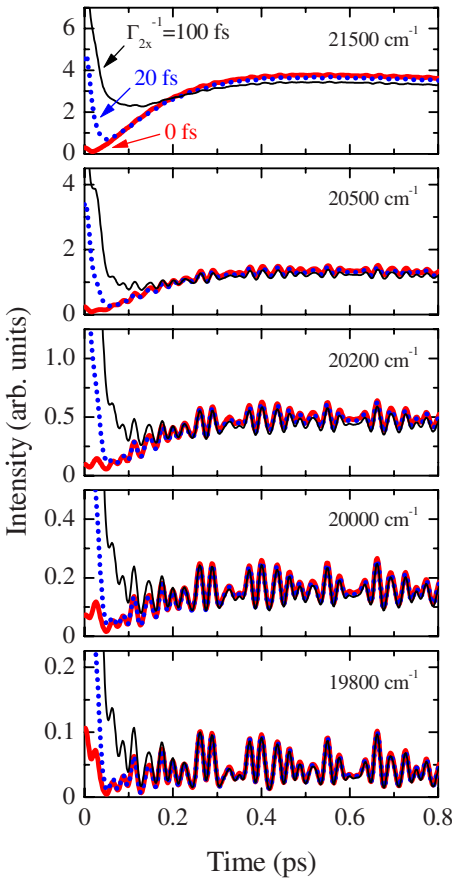

FIG. 9. (Color online) Excitation-energy dependence of TG signals calculated by systematically changing the S_2 to S_x internal conversion rate Γ_{2x}. Thick solid curve: $\Gamma_{2x}^{-1}=0$ fs (instantaneous relaxation). Thick dotted curve: $\Gamma_{2x}^{-1}=20$ fs. Thin solid curve: $\Gamma_{2x}^{-1}=100$ fs. The parameters used for calculation are the same as those for Fig. 6(b), but Γ_{x1}^{-1} is kept fixed at 120 fs.

cluded in the calculation. In each excitation energy the difference of the temporal intensity change in the TG signals is significant when $T<200$ fs. As one can clearly see in the curves using excitation at 21 500 cm^{-1} (top panel in Fig. 9), the intensity minimum shifts from 16 to 130 fs with the increase in Γ_{2x}^{-1}. It should be noted that these values of the minimum become larger when the influence of the coherent spike is included in the calculation. A similar trend can be seen in the curves calculated using other excitation energies. The dip becomes less pronounced as the excitation energy is decreased. In our experiment shown in Fig. 3(a), the minimum is located at about 40 fs in curves A and B. This is smaller than the value with the calculated TG curves in Fig. 9 with $\Gamma_{2x}^{-1}=20$ fs, where the minimum is located at 50 fs.[50] Since the excitation pulse of our experiment is 18 fs, this result suggests that shorter laser pulses are necessary in order to determine the time constant of the internal conversion from S_2 to S_x. It also indicates that our assumption that the instantaneous internal conversion from S_2 to S_x is reasonable under the present experimental conditions. We note that the dynamics on the S_2 potential surface is not clear at the present. To investigate this phenomenon, it is necessary to observe the TG signal by setting the pump energy at a much higher-energy region using much shorter optical pulses. However this experiment is not practical because of the intrinsically limited spectral range of the NOPA. We therefore leave this for the subject of future study.

The TG signals are also calculated by systematically changing Γ_{x1} while Γ_{2x}^{-1} is set constant at 20 fs. We found that when the decay rate Γ_{x1}^{-1} is set to 160 and 200 fs, the recovery of the signal is located at 650 and 800 fs, respectively. These are not consistent with the experiment. From this calculation, we conclude that the tolerance of Γ_{x1}^{-1} is about ± 20 fs.

Finally we briefly discuss the role of the S_x state. Our calculation suggests that the vibronic coherence excited in the S_2 state rapidly decays, while the vibronic oscillations in S_0 can be observed for more than 1 ps. We consider that the fast decay of the vibronic oscillations in S_2 is due to the relaxation into the S_x state because this is governed by a stochastic process.[52] As shown in Fig. 6(a) when the fast dephasing of the vibronic oscillation is not included in the calculation, the experimental results are not well reproduced. The key feature of our model is the existence of a singlet state, S_x, which facilitates the dephasing of the vibronic coherence that is initially excited in the S_2 state. The most plausible candidate for S_x may be an electronic state (e.g., $1B_u^-$ or $3A_g^-$) as theoretically pointed out by Tavan and Schulten.[21]

Another possible candidate for S_x might be a vibronically excited state of S_1. The C=C stretching mode coupled to the S_1 electronic state has a characteristic energy of about 1800 cm^{-1} and this is not observed in our FFT spectrum. However, this does not totally exclude the involvement of a vibrationally excited hot S_1 state in the relaxation process because the vibronic oscillations observed in the TG signals only reflect the *coherent* oscillations. The signal from hot S_1 would be expected to be detected in the slowly varying background in the present experimental setup because of the existence of the energy gap between S_1 and S_2. Therefore, the initial coherent oscillations in S_2 decay before the internal conversion to S_1 and it is reasonable for no information of hot S_1 to appear in the FFT spectrum. The calculated result indicates that the potentials between the S_2 and S_x are disjoint and that any coherent coupling between these states is very weak. Several authors have reported the vibrational cooling of hot S_1 with a time constant of about 400 fs,[37,53–55] which is somewhat longer than we have observed here, i.e., $\Gamma_{x1}^{-1}=120$ fs. Therefore, in the present case a possible involvement of a hot S_1 is less plausible. In any case, at the moment it is difficult to assign the origin of S_x with great certainty.

We note that Kukura *et al.*[19] have observed the stimulated Raman spectra of β-carotene, where the Raman modes coupled with the S_2 state have a full width at half maximum of 70 cm^{-1}. When a Lorentzian profile is assumed, the dephasing time is estimated to be 430 fs, which is much longer than the S_2-S_x time constant observed in the present study. This result suggests that the instantaneous relaxation from S_2 to S_x does not reflect the dephasing time of the vibronic coherent oscillations in the S_2 state.

Cerullo *et al.*[8] observed ultrafast optical response in the near-IR region, which was labeled as S_x with decays within 50 fs. As shown in Fig. 6(c), the TG signal is observed when

the electronic transition energy resonates with the pump energy. In the present experiment, since the pump energy was set in the visible region ($\sim$20 000 cm^{-1}), this ultrafast near-IR component was not detected. A more detailed study will be necessary to investigate the relationship between the instantaneous decay from S_2 to S_x investigated here and the ultrafast optical response reported in Ref. 8. This is left for future study. We note that the possible involvement of other singlet excited states, such as S^* and $S^{\ddagger}$, is unlikely because the lifetimes of these states are much longer than the time region investigated here.[5,25]

IV. SUMMARY

We have investigated the dynamics of the electronic excitation and vibronic coherent oscillations of β-carotene in THF by means of TG spectroscopy. It was found that the TG signal is very sensitive to the excitation energy. Following the coherent spike, the slowly varying background, reflecting the population dynamics, shows a large rise with a time constant of about 0.4 ps and then decays with a time constant of 5 ps when measured near the absorption maximum of the 0-0 transition. As the excitation energy decreases, the rise component becomes less prominent and the slowly varying background becomes weak. We calculated the TG signals at the various pump energies based on a Brownian oscillator model. Our model calculations suggest the existence of a singlet excited state between S_2 and S_1. It was found that the experimental results are better reproduced when instantaneous dephasing of the vibronic oscillation is assumed during the internal conversion from S_2 to S_x.

ACKNOWLEDGMENTS

This work was supported in part by the Grant-in-aid from the Japanese Ministry of Education, Culture, Sports, Science, and Technology (Grants No. 17654083, No. 18340091, and No. 18654074). R.J.C. acknowledges funding by the BBSRC. H.H. thanks Nissan Science Foundation for financial support.

*Corresponding author; mitsuru@sci.osaka-cu.ac.jp

[1] H. A. Frank and R. J. Cogdell, Photochem. Photobiol. **63**, 257 (1996).
[2] P. M. Champion, Science **310**, 980 (2005).
[3] V. Sundström, Annu. Rev. Phys. Chem. **59**, 53 (2008).
[4] H. van Amerongen, L. Valkunas, and R. van Grondelle, *Photosynthetic Excitons* (World Scientific, Singapore, 2000).
[5] As a review article, T. Polívka and V. Sundström, Chem. Rev. (Washington, D.C.) **104**, 2021 (2004).
[6] A. P. Shreve, J. K. Trautman, T. G. Owens, and A. C. Albrecht, Chem. Phys. Lett. **178**, 89 (1991).
[7] G. Cerullo, G. Lanzani, M. Zavelani-Rossi, and S. De Silvestri, Phys. Rev. B **63**, 241104(R) (2001).
[8] G. Cerullo, D. Polli, G. Lanzani, S. De Silvestri, H. Hashimoto, and R. J. Cogdell, Science **298**, 2395 (2002).
[9] T. Siebert, V. Engel, A. Materny, W. Kiefer, and M. Schmitt, J. Phys. Chem. A **107**, 8355 (2003).
[10] D. Kosumi, Y. Yanagi, T. Nishio, H. Hashimoto, and M. Yoshizawa, Chem. Phys. Lett. **408**, 89 (2005); D. Kosumi, M. Komukai, M. Yoshizawa, and H. Hashimoto, Phys. Rev. Lett. **95**, 213601 (2005).
[11] J. L. Pérez Lustres, A. L. Dobryakov, A. Holzwarth, and M. Veiga, Angew. Chem., Int. Ed. **46**, 3758 (2007).
[12] D. Polli, M. R. Antognazza, D. Brida, G. Lanzani, G. Cerullo, and S. De Silvestri, Chem. Phys. **350**, 45 (2008).
[13] H. Kandori, H. Sasabe, and M. Mimuro, J. Am. Chem. Soc. **116**, 2671 (1994).
[14] A. N. Macpherson and T. Gillbro, J. Phys. Chem. A **102**, 5049 (1998).
[15] S. Akimoto, I. Yamazaki, T. Sakawa, and M. Mimuro, J. Phys. Chem. A **106**, 2237 (2002).
[16] N. E. Holt, J. T. M. Kennis, and G. R. Fleming, J. Phys. Chem. B **108**, 19029 (2004).
[17] M. Yoshizawa, H. Aoki, M. Ue, and H. Hashimoto, Phys. Rev. B **67**, 174302 (2003).
[18] D. W. McCamant, P. Kukura, and R. A. Mathies, J. Phys. Chem. A **107**, 8208 (2003).
[19] P. Kukura, D. W. McCamant, and R. A. Mathies, J. Phys. Chem. A **108**, 5921 (2004).
[20] S. Shim and R. A. Mathies, J. Phys. Chem. B **112**, 4826 (2008).
[21] P. Tavan and K. Schulten, J. Chem. Phys. **85**, 6602 (1986); Phys. Rev. B **36**, 4337 (1987).
[22] See, for example, T. Sashima, H. Nagae, M. Kuki, and Y. Koyama, Chem. Phys. Lett. **299**, 187 (1999); T. Sashima, Y. Koyama, T. Yamada, and H. Hashimoto, J. Phys. Chem. B **104**, 5011 (2000); K. Furuichi, T. Sashima, and Y. Koyama, Chem. Phys. Lett. **356**, 547 (2002); F. S. Rondonuwu, Y. Watanabe, J. P. Zhang, K. Furuichi, and Y. Koyama, *ibid.* **357**, 376 (2002); R. Fujii, T. Inaba, Y. Watanabe, Y. Koyama, and J. P. Zhang, *ibid.* **369**, 165 (2003); K. Nishimura, F. S. Rondonuwu, R. Fujii, J. Akahane, Y. Koyama, and T. Kobayashi, *ibid.* **392**, 68 (2004); M. Ikuta, A. Yabushita, F. S. Rondonuwu, J. Akahane, Y. Koyama, and T. Kobayashi, *ibid.* **422**, 95 (2006); F. S. Rondonuwu, Y. Kakitani, H. Tamura, and Y. Koyama, *ibid.* **429**, 234 (2006).
[23] R. Fujii, T. Ishikawa, Y. Koyama, M. Taguchi, Y. Isobe, H. Nagae, and Y. Watanabe, J. Phys. Chem. A **105**, 5348 (2001); R. Fujii, T. Fujino, T. Inaba, H. Nagae, and Y. Koyama, Chem. Phys. Lett. **384**, 9 (2004).
[24] Y. Koyama, F. S. Rondonuwu, R. Fujii, and Y. Watanabe, Biopolymers **74**, 2 (2004); F. S. Rondonuwu, K. Yokoyama, R. Fujii, Y. Koyama, R. J. Cogdell, and Y. Watanabe, Chem. Phys. Lett. **390**, 314 (2004).
[25] H. Hashimoto, K. Yanagi, M. Yoshizawa, D. Polli, G. Cerullo, G. Lanzani, S. De Silvestri, A. T. Gardiner, and R. J. Cogdell, Arch. Biochem. Biophys. **430**, 61 (2004).
[26] D. Polli, G. Cerullo, G. Lanzani, S. De Silvestri, K. Yanagi, H. Hashimoto, and R. J. Cogdell, Phys. Rev. Lett. **93**, 163002 (2004).
[27] *Coherent Vibrational Dynamics*, edited by S. De Silvestri, G.

Cerullo, and G. Lanzani (CRC Press, Boca Raton, 2008).
[28] W. H. Zurek, Phys. Today **44** (10), 36 (1991).
[29] E. Joos, H. D. Zeh, C. Keiefer, D. Giulini, J. Kupsch, and I.-O. Stamatescu, *Decoherence and the Appearance of a Classical World in Quantum Theory* (Springer-Verlag, Berlin, 2003).
[30] A. Vagov, V. M. Axt, T. Kuhn, W. Langbein, P. Borri, and U. Woggon, Phys. Rev. B **70**, 201305(R) (2004).
[31] T. Itakura and Y. Tokura, Phys. Rev. B **67**, 195320 (2003).
[32] M. Bayer and A. Forchel, Phys. Rev. B **65**, 041308(R) (2002).
[33] C. R. Gonzalez, S. Fernandez-Alberti, J. Echave, and M. Chergui, J. Chem. Phys. **116**, 3343 (2002).
[34] See, for example, M. H. Vos, J.-C. Lambry, S. J. Robles, D. C. Youvan, J. Breton, and J. L. Martin, Proc. Natl. Acad. Sci. U.S.A. **88**, 8885 (1991); M. H. Vos, F. Rappaport, J. C. Lambry, J. Breton, and J. L. Martin, Nature (London) **363**, 320 (1993); M. H. Vos, M. R. Jones, C. N. Hunter, J. Breton, and J. L. Martin, Proc. Natl. Acad. Sci. U.S.A. **91**, 12701 (1994); T. Joo, Y. Jia, J.-Y. Yu, D. M. Jonas, and G. R. Fleming, J. Phys. Chem. **100**, 2399 (1996); R. Jimenez, F. van Mourik, J. Y. Yu, and G. R. Fleming, J. Phys. Chem. B **101**, 7350 (1997); W. M. Diffey, B. J. Homoelle, M. D. Edington, and W. F. Beck, *ibid.* **102**, 2776 (1998); S. Sporlein, W. Zinth, and J. Wachtveitl, *ibid.* **102**, 7492 (1998); R. Agarwal, M. Yang, Q.-H. Xu, and G. R. Fleming, *ibid.* **105**, 1887 (2001); V. I. Prokhorenko, A. R. Holzwarth, F. R. Nowak, and T. J. Aartsma, *ibid.* **106**, 9923 (2002); J. Konradi, A. K. Singh, A. V. Scaria, and A. Materny, J. Raman Spectrosc. **37**, 697 (2006); K. R. Shelly, E. C. Golovich, and W. F. Beck, J. Phys. Chem. B **110**, 20586 (2006); K. R. Shelly, E. C. Golovich, K. L. Dillman, and W. F. Beck, *ibid.* **112**, 1299 (2008).
[35] T. Hornung, H. Skenderović, and M. Motzkus, Chem. Phys. Lett. **402**, 283 (2005).
[36] J. Hauer, H. Skenderovik, K.-L. Kompa, and M. Motzkus, Chem. Phys. Lett. **421**, 523 (2006); J. Hauer, T. Buckup, and M. Motzkus, Chem. Phys. **350**, 220 (2008).
[37] J. Hauer, T. Buckup, and M. Motzkus, J. Phys. Chem. A **111**, 10517 (2007).
[38] M. Sugisaki, K. Yanagi, R. J. Cogdell, and H. Hashimoto, Phys. Rev. B **75**, 155110 (2007).
[39] M. Fujiwara, K. Yamauchi, M. Sugisaki, A. Gall, B. Robert, R. J. Cogdell, and H. Hashimoto, Phys. Rev. B **77**, 205118 (2008).
[40] N. Christensson, T. Polívka, A. Yartsev, and T. Pullerits, Phys. Rev. B **79**, 245118 (2009).
[41] As review articles on transient grating spectroscopy, see M. D. Fayer, Annu. Rev. Phys. Chem. **33**, 63 (1982); **52**, 315 (2001); B. I. Grimberg, V. V. Lozovoy, M. Dantus, and S. Mukamel, J. Phys. Chem. A **106**, 697 (2002).
[42] S. Saito and M. Tasumi, J. Raman Spectrosc. **14**, 299 (1983); S. Saito, M. Tasumi, and C. H. Eugster, *ibid.* **14**, 310 (1983).
[43] S. Schlücker, A. Szeghalmi, M. Schmitt, J. Popp, and W. Kiefer, J. Raman Spectrosc. **34**, 413 (2003).
[44] S. Mukamel, *Principles of Nonlinear Optical Spectroscopy* (Oxford University Press, New York, 1995).
[45] W. B. Bosma, Y. J. Yan, and S. Mukamel, Phys. Rev. A **42**, 6920 (1990).
[46] Y. J. Yan and S. Mukamel, J. Chem. Phys. **94**, 179 (1991).
[47] M. Sugisaki, M. Fujiwara, K. Yanagi, R. J. Cogdell, and H. Hashimoto, Photosynth. Res. **95**, 299 (2008).
[48] M. Cho, J.-Y. Yu, T. Joo, Y. Nagasawa, S. A. Passino, and G. R. Fleming, J. Phys. Chem. **100**, 11944 (1996); G. R. Fleming and M. H. Cho, Annu. Rev. Phys. Chem. **47**, 109 (1996).
[49] S. Akimoto, T. Tomo, Y. Naitoh, A. Otomo, A. Murakami, and M. Mimuro, J. Phys. Chem. B **111**, 9179 (2007).
[50] Recently Christensson *et al.* (Ref. 40) have reported the TG signals and photon-echo peak shifts of two carotenoids: astaxanthin and lycopene. The experimental results are analyzed based on the model proposed by Brixner *et al.* (Ref. 51), which is more rigorous than the model used in this study. The intermediate state S_x is not included in their model calculation, which appears to contradict with our results. The most important aspect of the present study is that the minimum around 50 fs shown in Fig. 3(a) is reproduced better only when an intermediate state between S_2 and S_1 is introduced (see Fig. 9).
[51] T. Brixner, T. Mančal, I. V. Stiopkin, and G. R. Fleming, J. Chem. Phys. **121**, 4221 (2004).
[52] When we assume that the coherence is conserved in the $S_2 \rightarrow S_x$ process and then lost subsequently in the $S_x \rightarrow S_1$ process, the TG signals should be the same as those shown in Fig. 6(a), but this does not reproduce the experimental results.
[53] F. L. de Weerd, I. H. M. van Stokkum, and R. van Grondelle, Chem. Phys. Lett. **354**, 38 (2002).
[54] T. Buckup, J. Savolainen, W. Wohlleben, J. L. Herek, H. Hashimoto, R. R. B. Correia, and M. Motzkus, J. Chem. Phys. **125**, 194505 (2006).
[55] P. O. Andersson and T. Gillbro, J. Chem. Phys. **103**, 2509 (1995).